Finno, R. (1994). *Géotechnique* **44**, No. 3, 545–550

DISCUSSION

Analytical interpretation of dilatometer penetration through saturated cohesive soils

R. FINNO (1993). *Géotechnique* **43**, No. 2, 241–254

A. J. Whittle, *Massachusetts Institute of Technology*

The Author has analysed the disturbance caused by dilatometer penetration in clay in order to establish factors affecting the contact pressure measurement p_0. In principle, these results can then be used to interpret proposed empirical correlations between the horizontal stress index $K_D = (p_0 - u_0)/\sigma_{v0}'$ (where u_0 and σ_{v0}' are the in situ pore water pressure and vertical effective stress, respectively) and engineering properties including K_0, OCR and s_u. The Author's analysis of penetration is based on the framework of the strain path method (Baligh, 1985) and estimates soil strains using a relatively complex simulation of the surface geometry through the superposition of spherical point sources. This technique is approximate and cannot model discontinuities such as the sharp edges of the dilatometer. Given these difficulties, the Author should clarify the exact geometry used in his analysis.

Similar studies of dilatometer performance at Massachusetts Institute of Technology (Whittle, Aubeny, Rafalovich, Ladd & Baligh, 1991; Aubeny, 1992; Rafalovich, 1991; Williamson, 1989) have been performed using a variety of strain path analyses. This research has shown that it is difficult to achieve accurate solutions of installation disturbance using boundary element methods (panel methods) to model the complete three-dimensional surface geometry. However, fundamental aspects of dilatometer penetration can be described using a simple plate geometry generated by a single line source of finite length (in a uniform flow).

Figure 12 shows the cartesian reference frame x, y, z ($x \equiv x_2$, $y \equiv x_1$) and geometry of a line source of finite length $2B$. The simple plate geometry is obtained by superimposing this fundamental solution on a uniform flow of velocity u_z which is equivalent to the rate of dilatometer penetration. The velocity components are given by

$$v_x = \frac{Q' \cos\theta}{4\pi r}\left\{\frac{\rho_1(y-B) - \rho_2(y+B)}{\rho_1\rho_2}\right\} \tag{1a}$$

$$v_y = \frac{Q'}{4\pi}\left\{\frac{\rho_1 - \rho_2}{\rho_1\rho_2}\right\} \tag{1b}$$

$$v_z = u_z + \frac{Q' \sin\theta}{4\pi r}\left\{\frac{\rho_1(y-B) - \rho_2(y+B)}{\rho_1\rho_2}\right\} \tag{1c}$$

where Q' is the source strength per unit length, and r, θ, ρ_1 and ρ_2 are all defined in Fig. 12.

The strain rates in the soil can also be expressed analytically by differentiation of the velocities with respect to the spatial co-ordinates

$$\dot{\varepsilon}_{xx} = \frac{Q'}{4\pi}\left[\left(\frac{\rho_1(y-B) - \rho_2(y+B)}{\rho_1\rho_2}\right)\left(\frac{1}{r^2} - \frac{2x^2}{r^4}\right) - \frac{x^2}{r^2}\left(\frac{\rho_1{}^3(y-B) - \rho_2{}^3(y+B)}{\rho_1{}^3\rho_2{}^3}\right)\right] \tag{2a}$$

$$\dot{\varepsilon}_{yy} = -\frac{Q'}{4\pi}\left(\frac{\rho_1{}^3(y-B) - \rho_2{}^3(y+B)}{\rho_1{}^3\rho_2{}^3}\right) \tag{2b}$$

$$\dot{\varepsilon}_{zz} = \frac{Q'}{4\pi}\left[\left(\frac{\rho_1(y-B) - \rho_2(y+B)}{\rho_1\rho_2}\right)\left(\frac{1}{r^2} - \frac{2z^2}{r^4}\right) - \frac{z^2}{r^2}\left(\frac{\rho_1{}^3(y-B) - \rho_2{}^3(y+B)}{\rho_1{}^3\rho_2{}^3}\right)\right] \tag{2c}$$

$$\dot{\varepsilon}_{xy} = -\frac{Q'x}{4\pi}\left(\frac{\rho_1{}^3 - \rho_2{}^3}{\rho_1{}^3\rho_2{}^3}\right) \tag{2d}$$

$$\dot{\varepsilon}_{yz} = -\frac{Q'z}{4\pi}\left(\frac{\rho_1{}^3 - \rho_2{}^3}{\rho_1{}^3\rho_2{}^3}\right) \tag{2e}$$

$$\dot{\varepsilon}_{zx} = -\frac{Q'}{4\pi}\left[\left(\frac{\rho_1(y-B) - \rho_2(y+B)}{\rho_1\rho_2}\right)\left(\frac{2xz}{r^4}\right) - \frac{xz}{r^2}\left(\frac{\rho_1{}^3(y-B) - \rho_2{}^3(y+B)}{\rho_1{}^3\rho_2{}^3}\right)\right] \tag{2f}$$

The strain paths of individual soil elements can be obtained accurately from equations (1) and (2) by numerical integration along streamlines. The width of the simple plate $2w$ for a given length $2B$ is controlled by the magnitude of the source strength Q' relative to the velocity of penetration u_z.

Figure 13 shows the deformations of the soil and geometry for a simple plate with aspect ratio

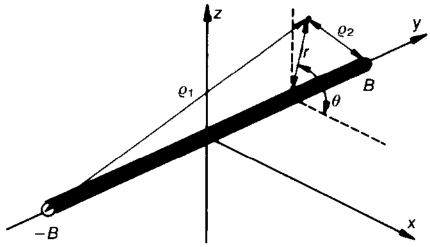

Fig. 12. Geometry of line source

$B/w = 6{\cdot}8$ which has the same cross-sectional area as the Marchetti dilatometer. The simple plate has a rounded tip geometry, smooth edges and infinite vertical extent, whereas the dilatometer has a sharp tip (20° apex angle), square cut edges and a total blade height $z/w \approx 34$. In spite of the apparent differences in geometry, the strain paths of the simple plate (Whittle *et al.*, 1991) are qualitatively similar to the results presented in Figs 3 and 4). Fig. 14 shows contours of the octahedral shear strain E around the simple plate in the vertical centre plane ($y = 0$) and in a horizontal (x–y) plane located far above the tip. These results show that soil strains stabilize at an elevation $z/w \geqslant 10$ above the tip, whereas average strain conditions are uniform longitudinally across the middle 40–50% of the plate face (i.e. $|y/w| \leqslant 3$–4). Fig. 15 compares the distribution of octahedral shear strain from the simple plate (Fig. 14(b)) with the results in Fig. 5, along the two planes of symmetry. Although the two solutions coincide in the centre plane ($y = 0$), they are in agreement only in the far field (i.e. large y/w) of the edge plane ($x = 0$). These results show that the shear behaviour in the far field is controlled primarily by the cross-sectional area of the dilatometer, whereas its surface geometry affects behaviour around the edge. Lack of smoothness in the contours of E (Fig. 5) may reflect numerical inaccuracies in the Author's solution.

Figure 16 summarizes the shear strain distribution of simple plates as a function of the aspect ratio B/w and the normalized lateral distance x/R_{eq}, where R_{eq} is the equivalent radius of an axisymmetric penetrometer

$$R_{eq} = \sqrt{(4Bw/\pi)} \tag{3}$$

For $x/R_{eq} \geqslant 10$–30, the shear strains caused by plate installation are independent of the aspect ratio (for $B/w = 6{\cdot}8$–$32{\cdot}5$) and correspond to the solutions for an axisymmetric penetrometer. The zone of disturbance can be estimated by comparing these results with the yield strain E_y (Baligh, 1986), which controls the extent of excess pore pressures in an isotropic soil. For most soft clays which yield at small strains ($E_y \leqslant 2{\cdot}0\%$), the results in Fig. 16 give a clear indication that the zone of disturbance around the dilatometer membrane ($R_{eq} = 20{\cdot}8$ mm) is very similar in magni-

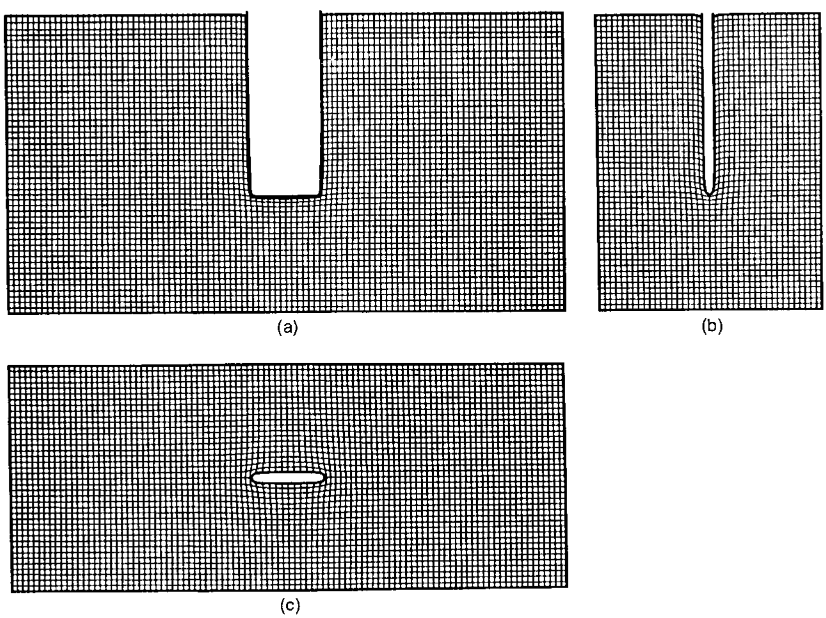

Fig. 13. Simple plate dilatometer

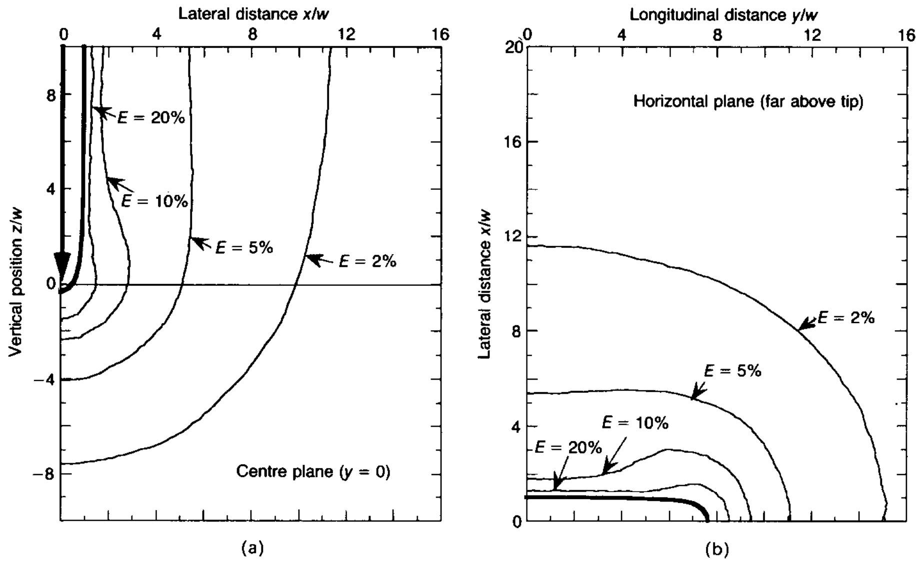

$$E = \sqrt{[(\varepsilon_{xx} - \varepsilon_{yy})^2 + (\varepsilon_{yy} - \varepsilon_{zz})^2 + (\varepsilon_{zz} - \varepsilon_{xx})^2 + 6(\varepsilon^2_{xy} + \varepsilon^2_{yz} + \varepsilon^2_{zx})] / 3}$$

Fig. 14. Shear strains around simple plate dilatometer, B/w = 6·8

tude to that around the shaft of a standard piezocone (axisymmetric, $R = 17{\cdot}8$ mm). This observation contradicts the Author's interpretation based on shear stress ratio (Fig. 7).

Excess pore pressures $\Delta u = u - u_0$ represent the major component of the contact pressure p_0 for dilatometer tests performed in normally and lightly overconsolidated clays. As a result, approximations in the computation of Δu within strain path analyses should be evaluated very carefully, and should be distinguished from parametric studies based on variations in measurable soil properties.

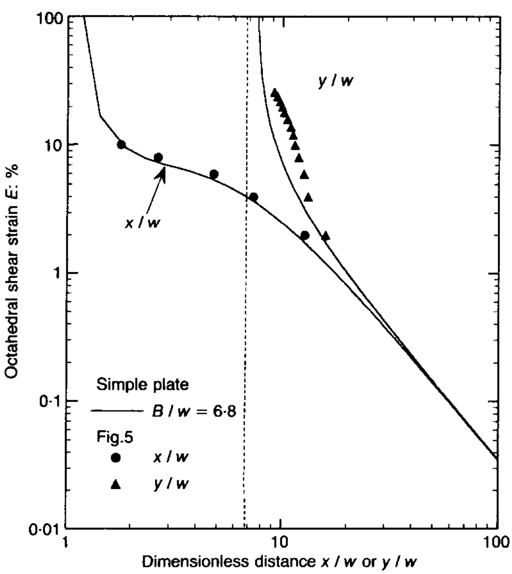

Fig. 15. Evaluation of strain solutions given in the Paper

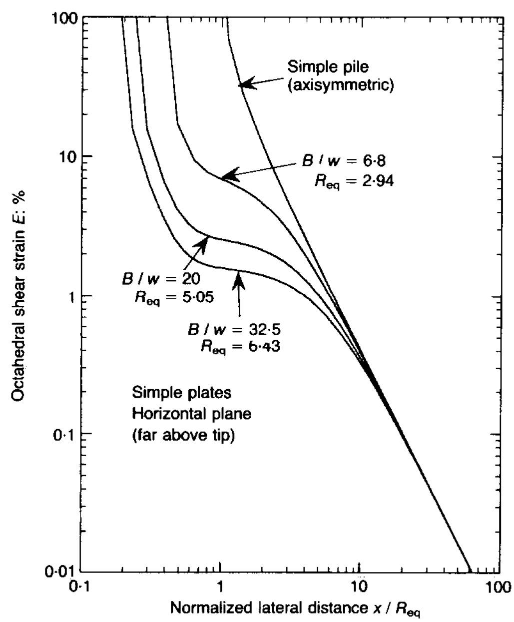

Fig. 16. Effect of plate aspect ratio on shear strain during installation

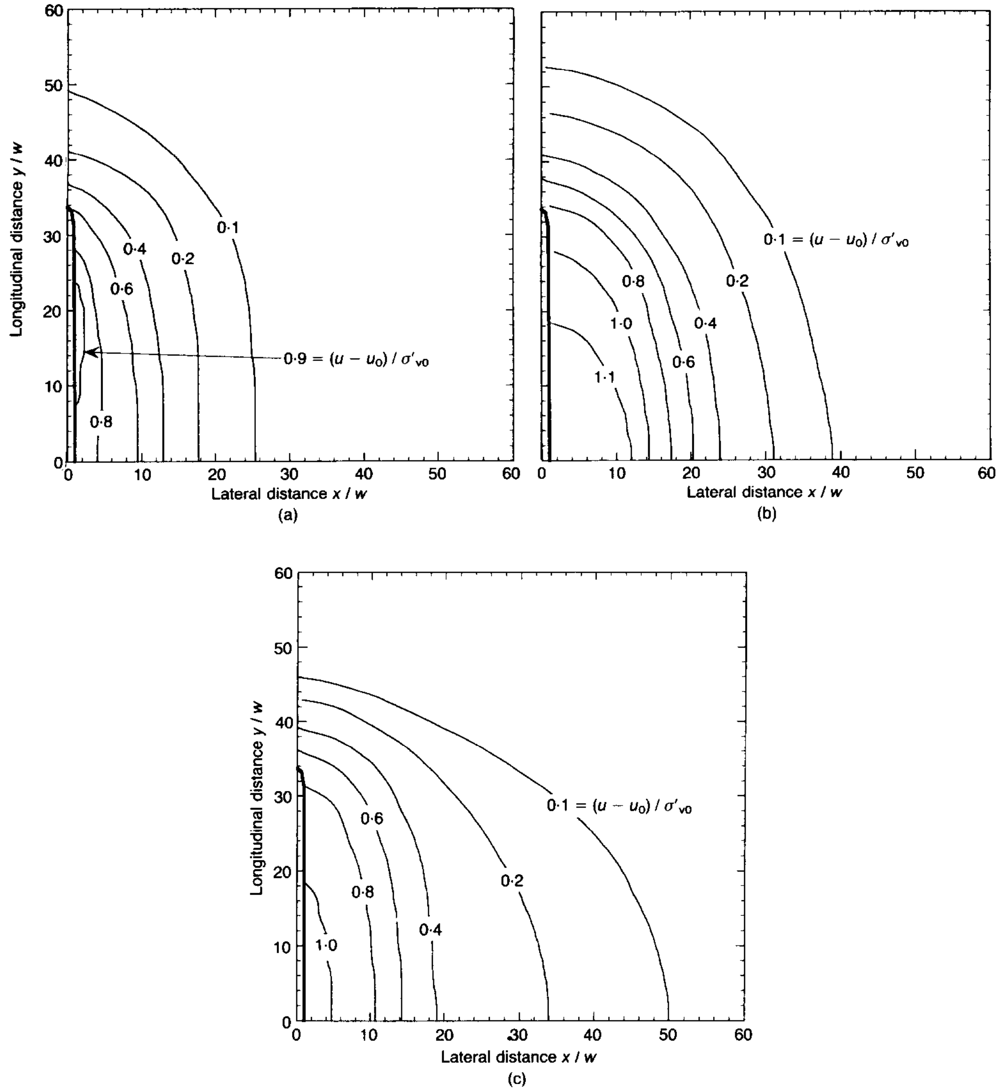

Fig. 17. Excess pore pressures around thin plate penetrometer; $B/w = 32{\cdot}5$, modified Cam clay, Boston blue clay: (a) integration in x direction; (b) integration in y direction; (c) solution of Poisson equation

Figures 17(a) and 17(b) show contours of excess pore pressure far above the penetrating tip of a thin simple plate penetrometer ($B/w = 32{\cdot}5$) which were computed by integration of the effective stress gradients in two orthogonal directions (the analyses use the modified Cam clay model with properties corresponding to K_0 normally consolidated Boston blue clay). The solutions presented in the Paper correspond closely to the x direction integration in Fig. 17(a). There are significant differences in both the magnitude of the excess pore pressure at the surface of the plate (25% variation) and also its spatial distribution due to the integration path.

Whittle *et al.* (1991) have recommended computing the excess pore pressures by solving the complete equilibrium conditions in the form of a Poisson equation. This method is rational and needs no subjective judgement in selecting the integration path. Fig. 17(c) shows that the Poisson equation generally provides an average of the two previous results in the vicinity of the plate, but predicts a larger lateral zone of excess pore pressures.

The Author is not able to obtain reliable solutions for Δu close to the surface of the dilatometer (within a zone approximately 10 mm thick). The results in Fig. 17 suggest that this limitation may not be important at locations around the dilatometer membrane. However, close to the tip of the dilatometer, there are very large gradients of excess pore pressures in both the lateral and vertical directions (x, z in Fig. 14) which can introduce significant errors in the computed behaviour in this region. For example, the Author predicts maximum excess pore pressures (Figs 6 and 10) at the base of the cone (i.e. at $x_3 \approx 4$ cm), whereas minimum values of Δu occur at the tip. These results are contrary to previous measurements for sharp-tipped piezocone penetrometers (Baligh & Levadoux, 1980) and deserve further investigation.

Author's reply

Professor Whittle makes the valid point that the estimates of soil strains using the approach of superposition of spherical point sources within the framework of the strain path method are approximate and presents the results of similar computations based on representing a penetrating dilatometer as a line source of finite length within a uniform flow field. In the solution presented in the Paper, a single spherical point source in a uniform flow field represents the penetration of a cylindrical object with a rounded point. As such the superposition of a number of these, even the 500 which model the dilatometer blade as shown in Fig. 1, does not represent an exact solution to the problem. In fact, neither my, nor Professor Whittle's, nor any other solution, such as the panel method (Huang, 1989) is an exact solution to the penetrating dilatometer problem. Although differences must necessarily exist in a comparison of any of these approximate solutions of the strain field, the various solutions give similar results in the area of the membrane, where the pressures are measured in dilatometer tests.

Professor Whittle rightly points out that the zone of disturbance around the dilatometer is similar in magnitude to that of a standard cone. He bases his observations on the assumption that yield will occur at small strains ($E_y \leqslant 2\%$) for soft clays. I based the extent of the disturbance zone on the extent of the failure zone, which is not the same as yield in the anisotropic bounding surface model in my analysis. Even with these dissimilar methods of defining the extent of disturbance, results of the two analyses are similar. In Professor Whittle's case, the extent of the disturbed zones in the dilatometer and the cone are approximately 85 mm, based on the results of Fig. 16 and assuming the zone of disturbance is defined by 2% strain at yield. If disturbance is defined at 1·5% strain at yield, then the disturbed zones would be 125 mm and 107 mm for the dilatometer and cone, respectively. In fact the definition of the disturbed zone has a large impact on its extent. The definition of 2% yield is rather arbitrary. For example, in field observations strain localization (presumably preceded by local yield) in lightly overconsolidated, soft to medium stiff Chicago clay was observed to begin at about 1% of octahedral shear strain (Finno & Nerby, 1989). Given that the computed extent of the disturbed zone near the dilatometer membrane varies between 100 mm and 110 mm (Fig. 7), the results of Professor Whittle's and my analyses are similar.

I also agree that approximations in the computation of Δu should be distinguished from parametric studies based on variation in measurable soil properties. Pore pressure predictions for the same loading based on different constitutive models will necessarily result in differences in predicted response. Professor Whittle uses modified Cam clay with properties from Boston blue clay whereas I used an anisotropic bounding surface model with parameters representative of Chicago clay. Although the index properties of these soils are similar, the models represent soil behaviour differently. The anisotropic bounding surface model allows irrecoverable deformations within the bounding surface. Modified Cam clay is isotropic and does not allow irrecoverable deformations within the yield surface. For a stress–strain history which includes a loading reversal (Fig. 8), significantly different response will be predicted by the two models. Therefore all differences in predicted pore pressures between the two models cannot be attributed to the differences in the predicted strains.

The focus of the Paper was to identify the parameters which most affect the P_0 reading in a dilatometer test. Although there are differences in computed strain fields depending on the method of analysis, there is substantial agreement, especially at the membrane location. In addition, the trends of computed versus observed K_d values with overconsolidation ratio in Fig. 9 indicate that the approach in the Paper gives reasonable results. The parameters in the model to which K_d is sensitive are related to the initial state of the soil in the ground relative to a stress surface which represents a change in behaviour from small to large strains (K_0 and OCR). K_d values computed from the results of a dilatometer test are therefore sensitive to these values and are likely to exhibit good empirical correlations with them. However, K_d was relatively insensitive to strength and deformation parameters. Because S_u

values are related to K_d values in standard dilatometer correlations, S_u is only as good as the empirical correlations based on OCR and thus site-specific correlations are needed for S_u values based on dilatometer tests.

REFERENCES

Aubeny, C. P. (1992). *Rational interpretation of in-situ tests in cohesive soils.* PhD thesis, Massachusetts Institute of Technology.

Baligh, M. M. (1985). Strain path method. *J. Geotech. Engng Div. Am. Soc. Civ. Engrs* **111,** GT9, 1108–1136.

Baligh, M. M. (1986). Undrained deep penetration. 1: Shear stresses. *Géotechnique* **36,** No. 4, 471–485.

Baligh, M. M. & Levadoux, J.-N. (1980). *Pore pressure dissipation after cone penetration.* Sea Grant Report, MITSG 80-13. Massachusetts Institute of Technology.

Huang, A.-B. (1989). Strain path analyses for arbitrary three-dimensional penetrometers. *Int. J. Numer. Analyt. Meth. Geomech.* **13,** 551–564.

Rafalovich, A. (1991). *The mechanics of plate penetration in clays.* MS thesis, Massachusetts Institute of Technology.

Whittle, A. J., Aubeny, C. P., Rafalovich, A., Ladd, C. C. & Baligh, M. M. (1991). *Prediction and interpretation of in-situ penetration tests in cohesive soils.* Research Report R91-01. Department of Civil Engineering, Massachusetts Institute of Technology.

Williamson, A. E. (1989). *The use of a panel method to predict disturbance due to penetrometer installation in clays.* MS thesis, Massachusetts Institute of Technology.